Adsorption characteristics of methylene blue onto the N-succinyl-chitosan-*g*-polyacrylamide/attapulgite composite

Qi Li*, Yahong Zhao*, Li Wang*,†, and Wang Aiqin**

*College of Material Science and Art Design, Inner Mongolia Agricultural University, Hohhot 010018, P. R. China
**Center of Eco-material and Green Chemistry, Lanzhou Institute of Chemical Physics,
Chinese Academy of Sciences, Lanzhou 730000, P. R. China

Abstract−N-succinyl-chitosan-*g*-polyacrylamide/attapulgite (NSC-*g*-PAM/APT) composite was applied as adsorbent for the removal of methylene blue (MB) from aqueous solution. The initial pH value of the dye solutions, the contact temperature, the contact time and the concentration of the dye solutions on adsorption capacity of the composite for MB dye were investigated. The adsorption kinetics and isotherms were also studied. It was shown that all the sorption processes were better fitted by pseudo-second-order equation and the Langmuir equation. The results indicated that the adsorption capacity of the composite was higher than those of chitosan (CTS) and attapulgite (APT). The desorption studies revealed that the composite provided the potential for regeneration and reuse after MB dye adsorption, which implied that the composite could be used as quite effective adsorbent for the removal of MB from aqueous solution.

Key words: N-succinyl-chitosan, Attapulgite, Composite, Adsorption, Methylene Blue

INTRODUCTION

Dye containing waste stream is one of the major toxic industrial waste. Various types of dyes are used in the process industries like textile, paints, pulp and paper, carpet and printing. The effluents containing dyes are highly colored and cause water pollution [1]. Methylene blue (MB) is the most commonly used substance for dying cotton, wood and silk. MB can cause eye burns, which may be responsible for permanent injury to the eyes of humans and animals. On inhalation, it can give rise to short periods of rapid or difficult breathing, while ingestion through the mouth produces a burning sensation and may cause nausea, vomiting, profuse sweating, mental confusion and methemoglobinemia [2]. Therefore, environmental legislation has imposed stringent limits on the concentrations of pollutants that may be discharged in aqueous effluents from dyestuff manufacturing and textile industries [3].

Many treatment methods have been developed to remove dyes from wastewater. These methods can be divided into physical, chemical and biological schemes. Although chemical and biological approaches are effective in removing dyes, they require special equipment and are usually energy intensive. Additionally, these processes often generate large amounts of byproducts. Therefore, the conventional treatments such as coagulation, flocculation and biological treatment are no longer able to achieve high quality treated water [4]. The adsorption process is well-known for its simple design and easy operation. It is inexpensive as compared with other physical and chemical processes. The adsorption technique has been used effectively for the removal of metallic pollutants [5-7] and dyes from wastewater [1,8-10].

Chitosan (CTS), a biopolymer of glucosamine, has exhibited a higher capacity for adsorption of colorant than activated carbon. It has undoubtedly been one of the most popular adsorbents for the removal of metal ions and dyes [11-14] and is widely used in wastewater treatment applications. The amino (-NH$_2$) and hydroxy (-OH) groups on CTS chains can serve as coordination and reaction sites [15-18]. In addition, the last decade has witnessed a growing interest in chemical modification of CTS and its derivatives to enhance their properties and consequently expand their potential applications [19-23]. Among various techniques of chemical modifications, the carboxyl dibutyryl derivative of CTS is very attractive. However, the carboxyl dibutyryl derivative of CTS is so easily soluble in water that cannot be separated from the wastewater. Therefore, several attempts have been made to develop insoluble and effective adsorbents.

Attapulgite (APT) is a crystalline hydrated magnesium silicate with a fibrous morphology, large specific surface area and moderate cation exchange capacity, which is beneficial for the adsorption of heavy metals and dyes [24,25]. In recent years, a series of composite hydrogels (such as Poly (acrylic acid)/organo-attapulgite [26], and starch phosphate-*g*-polyacrylamide/attapulgite [27]) based on APT with improved properties have been fabricated. It is well known to us that hydrogels are formed of three-dimensional cross-linked polymer networks of flexible chains, which are able to absorb and retain water and solute molecules. The porous structure networks allow solute diffusion through the hydrogel structure. As a rule, the superadsorbent possess anion functional groups, they can absorb and trap cationic dyes, such as MB [28]. In our previous study, chitosan-*g*-poly (acrylic acid)/montmorillonite(CTS-*g*-PAA/MMT) showed good adsorption for MB in aqueous solution [29]. To our knowledge, there is no research about the adsorption characteristics of MB onto the NSC-*g*-PAM/APT composite. Therefore, a novel NSC-*g*-PAM/APT composite hydrogel was synthesized by inverse suspension polymerization. The effect of the pH value of the dye solutions, the contact temperature, the contact time and the concen-

---

†To whom correspondence should be addressed.
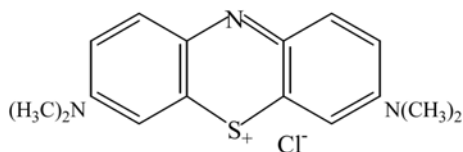E-mail: wl2083663@126.com

Fig. 1. Structure of MB.

tration of the dye solutions on the adsorption capacity of the NSC-g-PAM/APT composite for MB were studied and the adsorption mechanism and the reuse were also investigated in this paper.

EXPERIMENTAL

1. Materials

Acrylamide (AM, analytical grade, recrystallized from benzene before use), ammonium persulfate (APS, analytical grade, recrystallized from distilled water before use), N, N′-methylenebisacrylamide (MBA, analytical grade) and succinic anhydride (chemical grade) were supplied by Shanghai Reagent Corp. (Shanghai, China). Chitosan (CTS, degree of deacetylation is 0.85, average molecular weight is 90×10^4) was supplied by Zhejiang Yuhuan Ocean Biology Co. (Zhejiang, China). Attapulgite (APT, supplied by Linze Colloidal Co., Gansu, China) was milled through a 320-mesh screen and treated with 37% hydrochloric acid for 72 h, followed by washing with distilled water until pH=6 was achieved, and then dried at 105 °C for 8 h before use. Tween 80 (polyoxyethylene sorbitan monooleate) and Span80 (sorbitan monooleate) were purchased from Tianjin Reagent Corp. (Tianjin, China). The molecular formula of MB (Tianjin Reagent Corp., China) is $C_{16}H_{18}N_3SCl$ and the molecular structure is shown in Fig. 1. All the other reagents used were analytical grade and all solutions were prepared with distilled water.

2. Preparation of NSC-g-PAM/APT Composite and Their Characterization

The composite was prepared by the method of Li et al. [30]. The preparation procedure of NSC-g-PAM was similar to that of NSC-g-PAM/APT composite except without APT. The product was milled and the sample used for test was sieved through a 200-mesh screen. FTIR spectra (the sample was taken as KBr pellets using a Thermo Nicolet NEXUS TM spectrophotometer) showed that the graft reaction had taken place among NSC, AM and APT. The analysis of the micrographs (the sample was taken using SEM (JSM-5600LV, JEOL, Ltd.).) proved that there are really many micropores on the NSC-g-PAM/APT composite, which could be convenient for the penetration of dye into the network [30].

3. Adsorption Experiments

All batch adsorption experiments were performed on a thermostatted shaker (SHA-C) with a shaking of 120 rpm. During the effect of pH value on adsorption capacity of MB experiments, the MB solutions (640 mg/L) were adjusted to different pH values (2-12) with 0.10 mol/L NaOH or HCl solution using a pH meter (PB-10) and 0.10 g composite and 25.00 mL of MB solution were used at 30 °C for 30 min. The study of the influence of temperature on dye removed was carried out in the 25.00 mL of dye solution (800 mg/L, pH 6.00) with 0.10 g adsorbent for 30 min.

For kinetic study, 640 mg/L dye solutions (25.00 mL, pH 6.00) were agitated with 0.10 g adsorbent at 30 °C for predetermined inter-

vals of time. For isotherm study, batch adsorption equilibrium experiments were performed by agitating 25.00 mL various dye concentrations of MB solutions (pH 6.00) with 0.10 g adsorbent at 30 °C until equilibrium was reached.

The samples were withdrawn from the shaker at predetermined time intervals and the dye solutions were separated from the adsorbent by centrifugation at 8,000 r/min for 5 min. The adsorbencies of samples were measured with a UV-vis spectrophotometer (TU-1901) at 670 nm corresponding to a maximum adsorbency of MB. Then the concentrations of the samples were determined by using a linear regression equation (y=0.18439x+0.00282, R^2=0.9999) obtained by plotting a calibration curve for dye over a range of concentrations. The amounts of MB adsorbed onto samples were calculated by subtracting the final solution concentration from the initial concentration of dye solutions.

The amount of dye adsorbed at equilibrium q_e (mg/g) was calculated from the following equation:

$$q_e = \frac{(c_0 - c_e)v}{m} \qquad (1)$$

Where c_0 (mg/L) is the initial dye concentration, c_e (mg/L) is the equilibrium concentration of dye solution, v (L) the volume of dye solution, m (g) the mass of adsorbent.

4. Desorption Studies

For batch desorption study, the adsorbent utilized for the adsorption of c_0 of 640 mg/L was separated from the dye solution by centrifugation. The experiments were performed on a thermostatted shaker (SHA-C) with a shaking of 120 rpm. 0.10 g dye-loaded adsorbent and 25.00 mL of distilled water at different pHs were used at 30 °C for 30 min. The desorbed dye was determined as mentioned before.

RESULTS AND DISCUSSION

1. Effect of pH Value on Adsorption

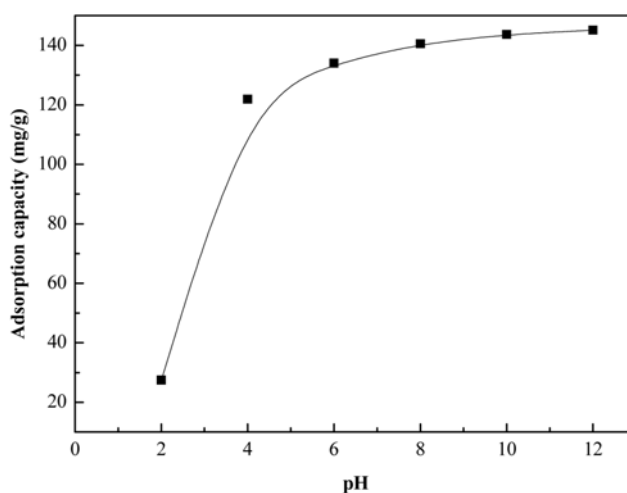The pH values of the dye solutions play an important role in the

Fig. 2. Effect of the pH values on adsorption capacity of NSC-g-PAM/APT for MB. Adsorption experiments-dye concentrations: 640 mg/L for NSC-g-PAM/APT composite; sample dose: 0.10 g/25.00 mL; pH rang: 2-12; temperature: 30 °C; equilibrium time: 30 min.

whole adsorption process and particularly on the adsorption capacity. Fig. 2 shows the effect of pH of dye solutions on the adsorption capacity of NSC-*g*-PAM/APT composite for MB. It can be seen from Fig. 2 that the adsorption capacity of composite increased sharply from 27 to 134 mg/g when the pH of dye solutions increased from 2 to 6, while the adsorption capacity increased continuously from 134 to 145 mg/g with further increasing pH of dye solutions from 6 to 12. This result may be attributed to the following reasons. At higher pH, most of the carboxylic groups in superadsorbent nanocomposite are ionized and interacting with the dye molecules, which results in an increase of the absorption for MB. In addition, at higher pH, the -COOH groups present in acrylate dissociate to form -COO, increasing the number of fixed ionized groups. This generates electrostatic repulsion forces among the adjacent ionized groups of polymer networks, inducing an expansion of the polymer chains within the superadsorbent nanocomposite structure, which also results in an increase of the absorption for MB. Similar result has been reported for the adsorption of MB by superadsorbent hydrogel formed by modified gum arabic, polyacrylate and polyacrylamide [28] and CTS-*g*-PAA/MMT nanocomposite [29].

2. Effect of Temperature on Adsorption

The relationship between the temperature and the adsorption capacity of MB onto the composite is shown in Fig. 3. It is found that the adsorption capacity of the composite increased from 134 mg/g to 191 mg/g with increasing temperature from 30 °C to 40 °C, and then decreased from 191 mg/g to 121 mg/g with further increase temperature from 40 °C to 70 °C. It is well known that increasing temperature may produce a swelling effect within the internal structure of adsorbent penetrating the large dye molecule further [31]. However, the mobility of the large dye ions increases with increasing temperature, which leads to a decrease in the adsorption capacity of composite with further increasing temperature [30]. Besides, the solubility of MB also increased, which caused the interaction forces between the solute and the solvent to become stronger than solute and adsorbent. Therefore, the solute was more difficult to
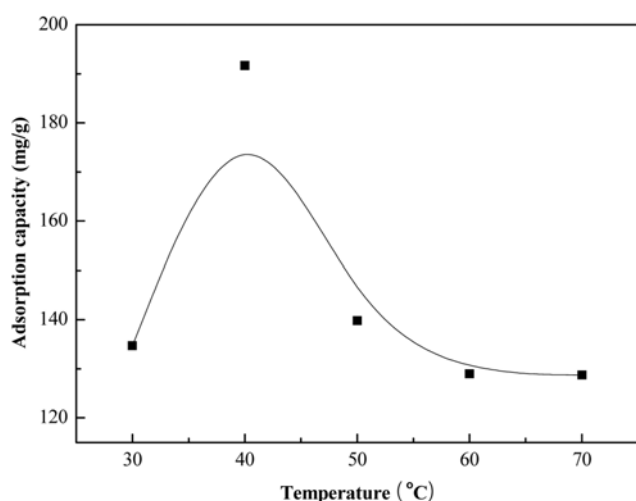

Fig. 3. Effect of the contact temperature on adsorption capacity of NSC-*g*-PAM/APT for MB. Adsorption experiments-dye concentrations: 800 mg/L for NSC-*g*-PAM/APT composite; sample dose: 0.10 g/25.00 mL; pH 6; temperature: 30-70 °C. equilibrium time: 30 min.
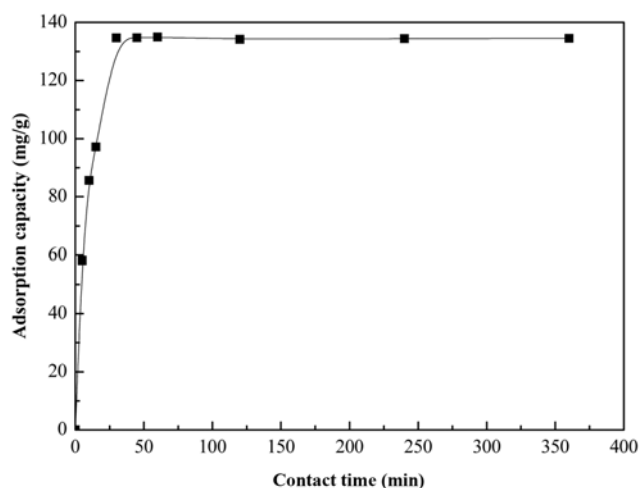
Fig. 4. Effect of the contact time on adsorption capacity of NSC-*g*-PAM/APT composite for MB. Adsorption experiments-dye concentrations: 640 mg/L for NSC-*g*-PAM/APT; sample dose: 0.10 g/25.00 mL; pH 6; temperature: 30 °C; adsorption time: 15, 30, 45, 60, 120, 240, 360 min.

adsorb [10].

3. Adsorption Kinetics

Contact time is an important parameter of adsorption, which can reflect the adsorption kinetics of an adsorbent. Fig. 4 shows the effect of contact time on the adsorption capacity of MB by the composite. It can be seen that the adsorption capacity of the composite increased rapidly in the initial stages of contact time and gradually increased with prolonging the contact time until equilibrium. It is clear that the adsorption equilibrium of the composite was reached at 30 min. So, in this study 30 min was chosen as the adsorption time to make sure the adsorption equilibrium was reached.

The adsorption kinetics can be explained by two simplified kinetics models: pseudo-first-order and pseudo-second-order equations. To investigate the controlling mechanism of adsorption process of NSC-*g*-PAM/APT composite for MB, the pseudo-first-order and the pseudo-second-order kinetic models were cited to evaluate the experimental data obtained from batch MB removal experiments.

The pseudo-first-order formula is given as [32]:

$$\frac{dq_e}{dt} = k_1(q_e - q_t) \qquad (2)$$

Where k_1 is the pseudo-first-order rate constant (min^{-1}), q_e and q_t are the amounts of dye adsorbed (mg/g) at equilibrium and time t (min).

After integration with the initial condition $q_t=0$ at $t=0$, Eq. (3) can be obtained:

$$\log(q_e - q_t) = \log q_e - \frac{k_1 t}{2.303} \qquad (3)$$

The pseudo-first-order kinetic model is valid only for the initial adsorption period [33,34]. Therefore, to find the potential rate-controlling steps involved in the adsorption processes of MB onto NSC-*g*-PAM/APT composite, the pseudo-second-order kinetic model was used to fit the experimental data.

Pseudo-second-order model is based on adsorption equilibrium

and it assumes that the rate-controlling step is chemisorption. It can be defined as [35]:

$$\frac{dq_e}{dt} = k_2(q_e - q_t)^2 \qquad (4)$$

When the initial condition is q_t=0 at t=0, Eq. (5) can be given as

$$\frac{t}{q_t} = \frac{1}{k_2 q_e^2} + \frac{t}{q_t} \qquad (5)$$

Where k_2 is the pseudo-second-order rate constant (g×mg^{-1}×min^{-1}), the linear plots of log $(q_e - q_t)$ versus t and (t/q_t) versus t drawn for the pseudo-first-order and the pseudo-second-order models, respectively. The rate constant of k_1 and k_2 can be obtained from the experimental data.

As seen from Figs. 5 and 6, the correlation coefficient (R^2) of the pseudo-first-order model is 0.9265. For the pseudo-second-order model, the correlation coefficient (R^2) is 0.9997. The linear R^2 coefficient (the coefficient of determination) compares the estimated and actual y-axis values and ranges in value from 0 to 1 when two
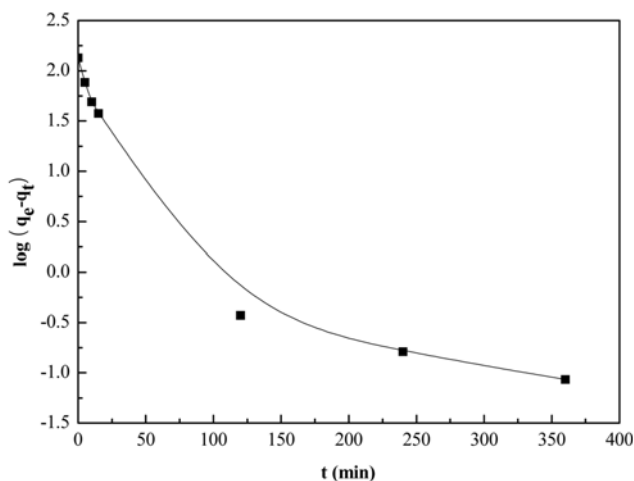

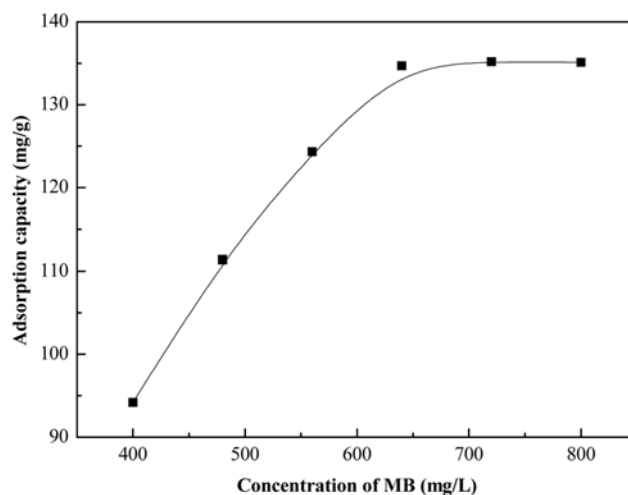Fig. 7. **Effect of the concentration of the dye solution on adsorption capacity of NSC-*g*-PAM/APT for MB. Adsorption experiments-sample dose: 0.10 g/25.00 mL; pH 6; temperature: 30 ºC; equilibrium time: 30 min.**

Fig. 5. **Pseudo-first-order model for the adsorption of MB by NSC-*g*-PAM/APT.**

Fig. 6. **Pseudo-second-order model for the adsorption of MB by NSC-*g*-PAM/APT.**

arrays of data are fitted to linear equation. If it is 1, there is a perfect correlation in the sample--there is no difference between the estimated and the actual y-axis value. At the other extreme, if the coefficient of determination is 0, the regression equation is not helpful in predicting a y-axis value. The non-linear R^2 value is based on the actual deviation between the experimental data and the theoretically predicted data and is a better correlation of the experimental data with the equation [33]. Therefore, the adsorption of MB on the composite was better described by the pseudo-second-order rather than by the pseudo-first-order.

4. Adsorption Isotherm

The influence of initial concentration on adsorption capacities of MB for the composite is shown in Fig. 7. It is clear that the concentration of dye solutions plays an important role in the adsorption capacity of dye onto adsorbent. It is can be seen that the adsorption capacity of the composite increased sharply from 94 mg/g to 134 mg/g with the initial concentrations of the dye increasing from 400 mg/L to 640 mg/L. However, the adsorption capacity hardly increased with further increasing the initial concentrations of the dye. Therefore, the equilibrium concentration of MB on the composite is 640 mg/L. These may be attributed to the following facts. On one hand, the higher initial MB concentration can lead to great driving force of the concentration gradient at the solid-liquid interface, and the increasing of the driving force may cause the increase of the amount of dyes ions adsorbed onto the adsorbent. On the other hand, the aggregation of MB dye molecules makes it almost impossible for them to diffuse deeper into NSC-*g*-PAM/APT composite structure [34,36].

Adsorption isotherms are important for the description of how molecules of adsorbate interact with adsorbent surface. The correlation of equilibrium data using either a theoretical or empirical equation is essential for the adsorption interpretation and prediction of the extent of adsorption [37]. The adsorption data is generally interpreted using the Langmuir and the Freundlich isotherm models. The Langmuir model is based on the assumption of a structurally homogeneous adsorbent where all adsorption sites are identical and

energetically equivalent. The Langmuir model is represented as follows [15]:

$$\frac{c_e}{q_e} = \frac{1}{bq_m} + \frac{c_e}{q_m} \qquad (6)$$

The Freundlich model is applied to describe heterogeneous system characterized by a heterogeneity factor of $1/n$. This model describes reversible adsorption and is not restricted to the formation of the monolayer. The Freundlich model is represented as follows [38]:

$$q_e = k_f c_e^{1/n} \qquad (7)$$

Where q_m (mg/g) and b (L/mg) are Langmuir isotherm coefficients. The value of q_m represents the maximum adsorption capacity, k_f (mg/g) and n are Freundlich constants.

The plots of c_e/q_e versus c_e and $\log q_e$ versus $\log c_e$, respectively are shown in Fig. 8 and Fig. 9. It is can be seen that the linearization of the equations and the correlation coefficients (R^2) of Langmuir and Freundlich models are $y=0.00743x-1.4354\times10^{-8}$, 1 and
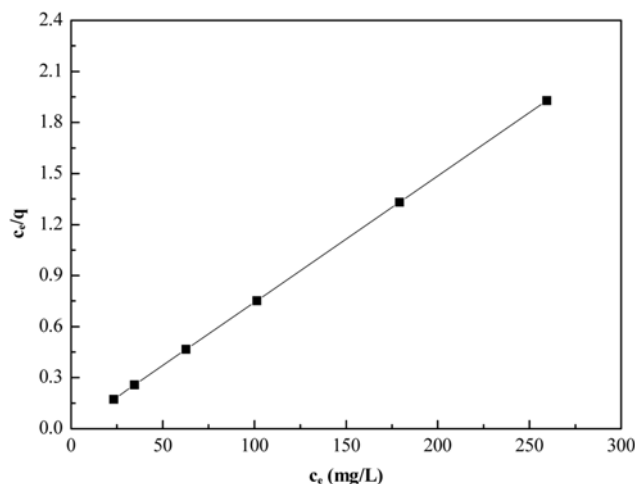
$y=0.1411x+1.8168$, 0.8190, respectively. In addition, the q_m value for the adsorption of MB by the composite was 135.14 mg/g, which is the same as the experiment data 134.57 mg/g for the composite. Obviously, compared with the Freundlich model, the Langmuir isotherm can be better fitted to the adsorption of MB on the composite. This means the monolayer coverage of the dye on the surface of the composite. Similar behaviors were also found for the adsorption of MB onto montmorillonite clay [39], carbon nanotubes [40], dehydrated peanut hull [41] and activated carbons from waste biomass by sulfuric acid activation [42]. The q_m values of MB on CTS-g-PAM/APT have been compared with those of other absorbents (Table 1). It can be seen that the q_m value of CTS-g-PAM/APT was much higher than that of other absorbents such as titanate nanotubes, crushed brick, garlic peel, APT, clay, CTS, coir pith carbon and raw powder of pyrophyllite. What is more, the introduction of APT clay also helps to reduce the market cost of CTS.

Table 1. The q_m values for the adsorption of MB on different adsorbents

Adsorbents	q_m (mg/g)	References
The citric acid modified wheat straw	396.9	[43]
NaOH-modified rejected tea	242.11	[44]
Cedar sawdust	142.36	[45]
NSC-g-PAM/APT	135.14	Our data in the paper
Titanate nanotubes	133.33	[46]
Crushed brick	96.61	[45]
Garlic peel	83	[47]
APT	68	Our data in the paper
Clay	58.2	[48]
CTS	36	Our data in the paper
Coir pith carbon	5.87	[49]
Raw powder of pyrophyllite	3.7	[50]

Fig. 8. Langmuir plot for the adsorption of MB by the NSC-g-PAM/APT composite.

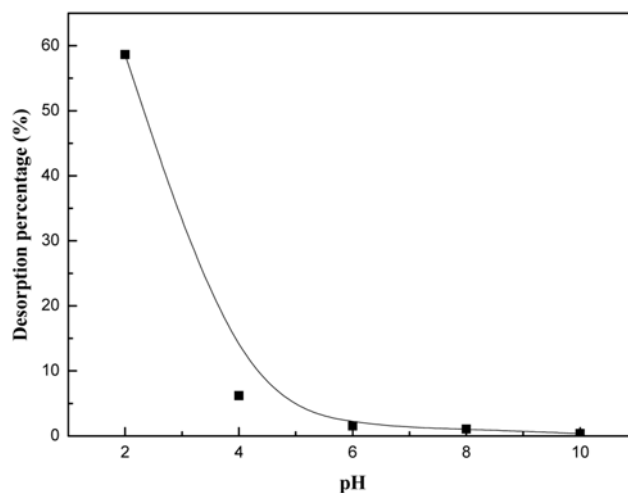**Fig. 9. Freundlich plot for the adsorption of MB by the NSC-g-PAM/APT composite.**

Fig. 10. Effect of pH on desorption percentage of dye from dye-loaded NSC-g-PAM/APT composite. Desorption experiments-dye concentrations: 640 mg/L for NSC-g-PAM/APT; sample dose: 0.10 g/25.00 mL; pH rang: 2-10; temperature: 30 ℃; equilibrium time: 30 min.

5. Desorption of MB

Desorption studies can help to regenerate the composite, so that it can be used again to adsorb the dye. Therefore, the recycling of the sorbent is a required step in the design of the process. Desorption studies can help in illustrating the mechanism of an adsorption process. If the dye adsorbed onto the adsorbent can be desorbed by water, it is can be said that the attachment of the dye on to the adsorbent is by weak bonds; if the strong acid (such as HNO_3 and HCl) can desorb the dye, it is believed that the contact of the dye on to the adsorbent is by ion exchange or electrostatic attraction [10]. Therefore, the distilled water with different pH values was used in the test; the effect of pH on desorption capacity of MB by the composite is shown in Fig. 10. The results indicate that the desorption capacity decreased rapidly with increasing of the pH; the lowest desorption capacity was 0.5 mg/g at pH 10, while in case of pH 2, 79 mg/g was obtained. It is clear that the adsorption of MB onto the composite was carried out significantly via electrostatic attraction. The results also indicate that the composite can be regenerated and reused after MB dye adsorption despite almost 40% dye remaining in the adsorbent in the case of pH 2.

CONCLUSIONS

The introduction of APT clay into NSC-g-PAM polymeric network could reduce the cost of adsorbents. The results showed that the adsorption capacity of the composite for MB is dependent on the initial pH value of the dye solutions, the contact temperature, the contact time and the concentration of the dye solutions. The results of the adsorption kinetics and isotherms showed that the adsorption processes of the composites for MB were all better fitted by the pseudo-second order equation and the Langmuir equation, respectively. The monolayer coverage of MB on the surface of the composites was in the ascendant. Compared with CTS and APT, the composite had a higher adsorption capacity. Furthermore, the desorption capacity of the composite nearly reached 60%. Therefore, the composite can be regenerated and reused, and can be effectively used as an adsorbent for the removal of MB from wastewaters.

ACKNOWLEDGEMENT

REFERENCES

1. P. Monash and G. Pugazhenthi, *Korean J. Chem. Eng.*, **27**, 1184 (2010).
2. D. Ghosh and K. G. Bhattacharyya, *Appl. Clay Sci.*, **20**, 295 (2002).
3. W. T. Tsai, C. Y. Chang, C. H. Ing and C. F. Chang, *J. Colloid Interface Sci.*, **275**, 72 (2004).
4. P. S. Kumar, S. Ramalingam and K. Sathishkumar, *Korean J. Chem. Eng.*, **28**, 149 (2011).
5. W. S. Wan Ngah and K. H. Liang, *Ind. Eng. Chem. Res.*, **38**, 1411 (1999).
6. J. Evans and P. T. Williams, *Process Saf. Environ.*, **78**, 40 (2000).
7. B. V. Babu and S. Gupta, *Adsorption.*, **14**, 85 (2008).
8. G. Mckay, M. E. I. Geundi and M. M. Nassar, *Process Saf. Environ.*, **74**, 277 (1996).
9. Y. S. Ho and G. Mckay, *Process Saf. Environ.*, **76**, 183 (1998).
10. I. A. W. Tan, A. L. Ahmad and B. H. Hameed, *J. Hazard. Mater.*, **154**, 337 (2008).
11. F. C. Wu, R. L. Tseng and R. S. Juang, *J. Hazard. Mater.*, **73**, 63 (2000).
12. K. H. Chu, *J. Hazard. Mater.*, **90**, 77 (2002).
13. W. S. Wan Ngah, A. Kamari, S. Fatinathan and P. W. Ng, *Adsorption.*, **12**, 249 (2006).
14. Y. C. Wong, Y. S. Szeto, W. H. Cheung and G. McKay, *Adsorption.*, **14**, 11 (2008).
15. I. Langmuir, *J. Am. Chem. Soc.*, **40**, 1361 (1918).
16. D. Knorr, *J. Food Sci.*, **48**, 36 (1983).
17. G. Mckay, H. S. Blair and J. R. Gardner, *J. Appl. Polym. Sci.*, **28**, 1767 (1983).
18. R. S. Juang, R. L. Tseng, F. C. Wu and S. H. Lee, *J. Chem. Technol. Biotechnol.*, **70**, 391 (1997).
19. M. Sugimoto, M. Morimoto, H. Sashiwa, H. Saimoto and Y. Shigemasa, *Carbohydr. Polym.*, **36**, 49 (1998).
20. H. Sashiwa and Y. Shigemasa, *Carbohydr. Polym.*, **39**, 127 (1999).
21. N. Terada, M. Morimoto, H. Saimoto, Y. Okamoto, S. Minami and Y. Shigemasa, *Chem. Lett.*, **28**, 85 (1999).
22. T. R. Sridhari and P. K. Dutta, *Indian J. Chem. Technol.*, **7**, 198 (2000).
23. A. Heras, N. M. Rodriguez, V. M. Ramos and E. Agullo, *Carbohydr. Polym.*, **44**, 1 (2001).
24. W. J. Wang, H. Chen and A. Q. Wang, *Sep. Purif. Technol.*, **55**, 157 (2007).
25. H. Chen and J. Zhao, *Adsorption.*, **15**, 381 (2009).
26. J. P. Zhang, H. Chen, P. Li and A. Q. Wang, *Macromol. Mater. Eng.*, **291**, 1529 (2006).
27. J. P. Zhang, A. Li and A. Q. Wang, *Carbohydr. Polym.*, **65**, 150 (2006).
28. A. T. Paulino, M. R. Guilherme, A. V. Reis, G. M. Campese, E. C. Muniz and J. Nozaki, *J. Colloid Interface Sci.*, **301**, 55 (2006).
29. L. Wang, J. P. Zhang and A. Q. Wang, *Colloids Surf. A: Physicochem. Eng. Aspects*, **32**, 47 (2008).
30. P. Li, J. P. Zhang and A. Q. Wang, *Macromol. Mater. Eng.*, **292**, 962 (2007).
31. K. G. Bhattacharyya and A. Sarma, *Dyes Pigm.*, **57**, 211 (2003).
32. S. Lagergren, *Kungl. Sven. Veten. Akad. Handl.*, **24**, 1 (1898).
33. I. D. Mall, V. C. Srivastava, G. V. A. Kumar and I. M. Mishra, *Colloids Surf. A: Physicochem. Eng. Aspects*, **278**, 175 (2006).
34. V. C. Srivastava, M. M. Swamy, I. D. Mall, B. Prasad and I. M. Mishra, *Colloids Surf. A: Physicochem. Eng. Aspects*, **272**, 89 (2006).
35. Y. S. Ho and G. McKay, *Process Biochem.*, **34**, 451 (1999).
36. I. D. Mall, V. C. Srivastava, N. K. Agarwal and I. M. Mishra, *Chemosphere*, **61**, 492 (2005).
37. E. L. Grabowska and G. Gryglewicz, *Dyes Pigm.*, **74**, 34 (2007).
38. H. M. F. Freundlich, *Z. Phys. Chem.*, **57**, 385 (1906).
39. C. A. P. Almeida, N. A. Debacher, A. J. Downs, L. Cottet and C. A. D. Mello, *J. Colloid Interface Sci.*, **332**, 46 (2009).
40. Y. J. Yao, F. F. Xu, M. Chen, Z. A. Xu and Z. W. Zhu, *Bioresour. Technol.*, **102**, 3040 (2010).
41. D. Özer, D. Gülbeyi and A. Özer, *J. Hazard. Mater.*, **144**, 171 (2007).

42. S. Karagöza, T. Tayb, S. Ucara and M. Erdemb, *Bioresour. Technol.*, **99**, 6214 (2008).

43. R. P. Han, L. J. Zhang, C. Song, M. M. Zhang, H. M. Zhu and L. J. Zhang, *Carbohydr. Polym.*, **79**, 1140 (2010).

44. N. Nasuha and B. H. Hameed, *Chem. Eng. J.*, **166**, 783 (2011).

45. H. Oualid, *J. Hazard. Mater.*, **135**, 264 (2006).

46. L. Xiong, Y. Yang, J. X. Mai, W. L. Sun, C. Y. Zhang, D. P. Wei, Q. Chen and J. R. Ni, *Chem. Eng. J.*, **156**, 313 (2010).

47. B. H. Hameed and A. A. Ahmad, *J. Hazard. Mater.*, **164**, 870 (2009).

48. A. Gürses, Ç. Doğar, M. Yalçın, M. Açıkyıldız, R. Bayrak and S. Karaca, *J. Hazard. Mater.*, **131**, 217 (2006).

49. D. Kavitha and C. Namasivayam, *Bioresour. Technol.*, **98**, 14 (2007).

50. J. W. Sheng, Y. N. Xie and Y. Zhou, *Appl. Clay Sci.*, **46**, 422 (2009).